

Resonance Raman Spectroscopic Detection of Both Linear and Bent Fe–CN Fragments for the Cyanide Adducts of Cytochrome P-450 Camphor and Its Substrate-Bound Forms. Relevance to the “Charge Relay” Mechanism

Mihaela C. Simianu and James R. Kincaid*

Contribution from the Chemistry Department, Marquette University, Milwaukee, Wisconsin 53233

Received August 22, 1994[⊗]

Abstract: The resonance Raman spectra of the cyanide adducts of cytochrome P-450 camphor in the substrate-free, camphor-bound, and adamantanone-bound forms are reported. Careful analyses of the difference patterns obtained by subtraction of various pairs of spectra of four CN[−] isotopomers provide convincing evidence for the presence of two structural conformers: one “essentially linear” and the other bent. Both conformers persist for the substrate-bound derivatives. The linear conformer exhibits the $\nu(\text{Fe}-\text{C})$ stretching mode at 413 cm^{−1} and the $\delta(\text{FeCN})$ bending mode at 387 cm^{−1} for the substrate-free derivative. The corresponding values for the camphor-bound form are 416 and 392 cm^{−1}, while for the adamantanone derivative these occur at 423 and 387 cm^{−1}. The bent conformer exhibits a set of vibrational parameters which is characterized by a “zigzag” isotope shift pattern for both the lower frequency and the higher frequency mode. For the substrate-free form, the vibrational modes of both conformers are shown to be sensitive to ¹H₂O/²H₂O exchange, confirming that they are both hydrogen bonded. While in the case of the linear conformer the H-bond donor is most likely the active site water cluster, the (presumably off-axis) donor for the bent conformer may be either another region of the water cluster or the threonine-252 (or aspartate-251) residue which may be in a position to interact with the polar CN[−] ligand. The vibrational frequencies of both conformers are sensitive to substrate binding and to the substrate size. Furthermore, the vibrational modes of both conformers are insensitive to ¹H₂O/²H₂O exchange in the substrate-bound forms. While the lack of ¹H₂O/²H₂O sensitivity does not exclude the possibility that one or both conformers are H-bonded, its absence, together with the demonstrated sensitivity to substrate size, suggests that steric factors are important in determining the geometry of the FeCN fragment. Finally, all the experimentally derived frequencies and isotopic shifts are shown to be consistent with the predictions of normal mode calculations for these two conformers.

Introduction

Cytochrome P450cam, which catalyzes the hydroxylation of camphor in the bacterium *Pseudomonas putida*, accomplishes the regio- and stereospecific hydroxylation of its substrate, *d*-camphor, at the 5-exo position.¹ The structure of this enzyme has been fairly well-defined by many spectroscopic studies^{2,4} and also by X-ray crystallography^{3a–f} for both the substrate-free and substrate-bound forms. The heme iron is axially coordinated by thiolate ligation involving the cysteine-357 residue. In the substrate-free form the distal pocket is occupied by a cluster of hydrogen-bonded water molecules which provides a water molecule (or hydroxide ion) as a sixth axial ligand, coordination of which results in a low-spin ferric heme iron.^{3a}

[⊗] Abstract published in *Advance ACS Abstracts*, April 15, 1995.

(1) (a) Yu, C.-A.; Gunsalus, I. C.; Katagiri, M.; Suhara, K.; Takemori, S. *J. Biol. Chem.* **1974**, *249*, 94–101. (b) Sligar, S. G. *Biochemistry* **1976**, *15*, 5399–5406. (c) Sato, R.; Omura, T. In *Cytochrome P450*; Sato, R., Omura, T., Eds.; Academic Press: New York, 1978. (d) Sligar, S. G.; Murray, R. I. In *Cytochrome P450*; Ortiz de Montellano, P. R., Ed.; Plenum Press: New York, 1986; pp 429–503. (e) Unger, B. P.; Sligar, S. G.; Gunsalus, I. C. In *The Bacteria*; Gunsalus, I. C., Steiner, R. I., Eds.; Academic Press: New York, 1986; Vol. X, pp 557–589.

(2) (a) O’Keefe, D. H.; Ebel, R. E.; Peterson, J. A.; Maxwell, J. C.; Caughey, W. S. *Biochemistry* **1978**, *17*, 5845–5852. (b) Lipscomb, J. D. *Biochemistry* **1980**, *19*, 3590–3599. (c) Dawson, J. H.; Andersson, L. A.; Sono, M. *J. Biol. Chem.* **1982**, *257*, 3606–3617. (d) Sono, M.; Dawson, J. H. *J. Biol. Chem.* **1982**, *257*, 5496–5502. (e) Sono, M.; Andersson, L. A.; Dawson, J. H. *J. Biol. Chem.* **1982**, *257*, 8308–8320. (f) Dawson, J. H.; Eble, K. S. In *Advances in Inorganic and Bioinorganic Mechanisms*; Academic Press: New York, 1985; Vol. 4, pp 1–64. (g) Shiro, Y.; Iizuka, T.; Makino, R.; Ishimura, Y.; Morishima, I. *J. Am. Chem. Soc.* **1989**, *111*, 7707–7711. (h) Banci, L.; Bertini, I.; Marconi, S.; Pierattelli, R. *Eur. J. Biochem.* **1993**, *215*, 431–437.

Upon binding of substrate, the water cluster is disrupted, destabilizing hexacoordination, and a high-spin ferric heme is produced, which is more readily reduced than its low-spin counterpart.¹ The substrate is held in an appropriate orientation via a “lock-and-key” hydrophobic contact between its C-8 and C-9 methyl groups and Leu-244, as well as a hydrogen-bonding interaction between its carbonyl oxygen and the phenol hydroxy group of Tyr-96.^{3b}

(3) (a) Poulos, T. L.; Finzel, B. C.; Howard, A. J. *Biochemistry* **1986**, *25*, 5314–5322. (b) Poulos, T. L.; Finzel, B. C.; Howard, A. J. *J. Mol. Biol.* **1987**, *195*, 687–700. (c) Raag, R.; Poulos, T. L. *Biochemistry* **1989**, *28*, 917–922. (d) Raag, R.; Poulos, T. L. *Biochemistry* **1991**, *30*, 2674–2684. (e) Raag, R.; Martinis, S. A.; Sligar, S. G.; Poulos, T. L. *Biochemistry* **1991**, *30*, 11420–11429. (f) Raag, R.; Li, H.; Jones, B. C.; Poulos, T. L. *Biochemistry* **1993**, *32*, 4571–4578. (g) Deatherage, J. F.; Loe, R. S.; Anderson, C. M.; Moffat, K. *J. Mol. Biol.* **1976**, *104*, 687–706. (h) Steigemann, W.; Weber, E. *J. Mol. Biol.* **1979**, *127*, 309–338. (i) Poulos, T. G.; Freer, S. T.; Alden, R. A.; Xuong, N. H.; Edwards, S. L.; Hamlin, R. C.; Kraut, J. In *J. Biol. Chem.* **1978**, *253*, 3730–3735. (j) Edwards, S. L.; Poulos, T. L. In *J. Biol. Chem.* **1990**, *265*, 2588–2595.

(4) (a) Champion, P. M.; Gunsalus, I. C.; Wagner, G. C. *J. Am. Chem. Soc.* **1978**, *100*, 3743–3751. (b) Champion, P. M.; Stallard, B. R.; Wagner, G. C.; Gunsalus, I. C. *J. Am. Chem. Soc.* **1982**, *104*, 5469–5472. (c) Uno, T.; Nishimura, Y.; Makino, R.; Iizuka, T.; Ishimura, Y.; Tsuboi, M. *J. Biol. Chem.* **1985**, *260*, 2023–2026. (d) Bangcharoenpaupong, O.; Krizos, A.; Champion, P. M.; Jollie, D.; Sligar, S. G. *J. Biol. Chem.* **1986**, *261*, 8089–8092. (e) Bangcharoenpaupong, O.; Champion, P. M.; Martinis, S.; Sligar, S. G. *J. Chem. Phys.* **1987**, *87*, 4273–4284. (f) Tsuboi, M. *Indian J. Pure Appl. Phys.* **1988**, *26*, 188–191. (g) Champion, P. M. In *Biological Applications of Raman Spectroscopy*; Spiro, T. S., Ed.; John Wiley & Sons: New York, 1988; Vol. 3, pp 249–292. (h) Egawa, T.; Ogura, T.; Makino, R.; Ishimura, Y.; Kitagawa, T. *J. Biol. Chem.* **1990**, *266*, 10246–10248. (i) Hu, S.; Schneider, A. J.; Kincaid, J. R. *J. Am. Chem. Soc.* **1991**, *113*, 4815–4822. (j) Hu, S.; Kincaid, J. R. *J. Am. Chem. Soc.* **1991**, *113*, 9760–9766. (k) Wells, A. V.; Li, P.; Champion, P. M.; Martinis, S. A.; Sligar, S. G. *Biochemistry* **1992**, *31*, 4384–4393.

The last detectable intermediate in the enzymatic cycle is a low-spin ternary complex involving the dioxygen adduct of the ferrous heme of the substrate-bound enzyme. Recent attention has focussed on a “charge relay” mechanism for O–O bond scission which incorporates a hydrogen bond interaction between the bound dioxygen and the ROH side chain of the nearby Thr-252 residue.⁵

Obviously, it is highly desirable to develop spectroscopic probes of such active site interactions so as to provide an effective means to monitor subtle differences associated with substrate structure or other environmental changes. Resonance Raman spectroscopy is now well established as such a method, the spectra providing detailed structural information for the heme moiety as well as axial ligand disposition.⁶ With regard to the issue of interest here (the proposed hydrogen bonding interaction of bound O₂ with distal side residues), problems arise because of the high reactivity of the ternary dioxygen adduct intermediate. While the corresponding adducts of other potential ligands, such as CO and NO, are relatively stable, these ligands are weaker H-bond acceptors and are less likely to participate in such interactions with relatively weak H-bond donors such as the threonine. In order to address this issue we have conducted a detailed RR study of the complex of ferric cytochrome P450cam with cyanide, a negatively charged ligand whose H-bond acceptor properties are expected to be more closely similar to that of ferrous-bound dioxygen (which is more properly formulated as a ferric–superoxo complex⁷).

Several RR studies of cyanide adducts of various heme proteins have been reported.⁸ In the absence of steric or electronic factors which destabilize a linear geometry, the Fe–C–N angle is expected to be ~180° and the non-totally symmetric $\delta(\text{FeCN})$ bending mode is formally RR inactive. Slight distortions of the Fe–CN fragment (bending or tilting) activate the bending mode and both it and the $\nu(\text{Fe–C})$ stretching mode are observable in the RR spectrum. In the case of model compounds, where the FeCN fragment is apparently strictly linear, only the stretching mode is observed.^{8b} However, the steric and/or H-bonding interactions present in the active sites of various heme proteins are apparently adequate to distort the FeCN fragment to the extent that both modes are activated.

Slight distortions give rise to an “essentially linear” form whose vibrational spectrum exhibits two modes which are sensitive to isotopic substitution of the CN[–] ligand. The higher frequency mode shifts monotonically with the total mass of the

ligand, the frequencies for the ¹³C¹⁴N[–] and ¹²C¹⁵N[–] isotopomers being identical, while the lower frequency mode exhibits a so-called “zigzag” pattern,^{6b} shifting only with isotopic substitution of the carbon atom. This pattern was observed in early studies of the CN[–] adducts of various oxygen transport proteins where a monotonically shifting $\nu(\text{Fe–C})$ was observed near 450 cm^{–1} along with the bending mode near 420 cm^{–1}, which exhibited the expected “zigzag” pattern.^{8a}

In some cases the distal pocket interactions are apparently of sufficient strength to induce a large off-axis distortion. In this situation the stretching and bending coordinates become kinematically coupled with the result that the mode energies are driven apart. This so-called “bent” conformation is characterized by a much larger separation of the two isotope sensitive modes and a reversal of their isotopic shift patterns.^{8c–h} Thus, the higher frequency mode exhibits a “zigzag” pattern while the lower frequency mode shifts monotonically with the total mass of the CN[–] ligand. Such a bent conformation was observed by Babcock and co-workers for the CN[–] adduct of myeloperoxidase, which exhibits a monotonically shifting mode at ~350 cm^{–1} and a higher frequency mode (~453 cm^{–1}) which shifts only upon substitution of the carbon atom.^{8d} Essentially identical results were obtained by Hu et al. for the cyanide adduct of lactoperoxidase.^{8e} Spiro and co-workers were the first to document the possibility that a heme protein–cyanide adduct can interconvert between the “essentially linear” and bent forms, observing both forms for the cyanide adduct of sulfite reductase.^{8c} Subsequently, the simultaneous existence of both forms has been documented for the cyanide adducts of horseradish peroxidase,^{8f} yeast cytochrome *c* peroxidase,^{8h} and two catalases.^{8g}

Evidence for such distortions is provided by crystal structures which are available for the cyanide adducts of several heme proteins.^{3g–j} Thus, in the case of cyanomethemoglobin^{3g} the cyanide ligand assumes a 20° tilt, whereas for the cyanide adduct of erythrocyruorin^{3h} the FeCN fragment was reported to have a distortion wherein the $\angle\text{Fe–C–N}$ is 165° and the $\angle\text{NpFeC}$ = 85°. In the case of the structure of the cyanide adduct of cytochrome *c* peroxidase,^{3i,j} it is reported that the difference electron density maps could be modeled with either a bent configuration ($\angle\text{Fe–C–N}$ = 130°) or one having the linear FeCN fragment tilted (i.e., $\angle\text{NpFeC}$ = 80°) from the heme normal. Significantly, recent RR results reported for this species suggest that both conformers are present in solution.^{8h}

In the present case, the RR data (along with a supporting normal mode calculation) confirm the presence of two conformers, one essentially linear and the other bent, for both the substrate-free and substrate-bound forms. The possible steric and electronic factors which control the disposition of the bound cyanide ligand are probed by conducting studies with two different sized substrates and ¹H₂O/²H₂O exchange and the results are discussed with reference to the recently proposed “charge relay” mechanism for O–O bond heterolysis.⁵

Experimental Procedures

Materials and Methods. Cytochrome P450cam (P450cam) was isolated and purified from *Pseudomonas putida* (ATCC 29607) cells grown on camphor as the sole hydrocarbon source. The method used was that described by Anderson,⁹ which is based on the method originally developed by Gunsalus and co-workers.¹⁰ Fractions with $R_z(A_{392}/A_{280}) > 1.5$ have been used for the resonance Raman measurements.

(9) Anderson, L. Ph.D. Dissertation, 1982, University of South Carolina.

(10) Gunsalus, I. C.; Wagner, G. C. In *Methods in Enzymology*; Fleischer, S., Packer, L., Eds.; Academic Press: New York, 1978; Vol. 52, pp 166–188.

(5) (a) Martinis, S. A.; Atkins, W. M.; Stayton, P. S.; Sligar, S. G. *J. Am. Chem. Soc.* **1989**, *111*, 9252–9253. (b) Gerber, N. C.; Sligar, S. G. *J. Am. Chem. Soc.* **1992**, *114*, 8742–8743. (c) Aikens, J.; Sligar, S. G. *J. Am. Chem. Soc.* **1994**, *116*, 1143–1144. (d) Gerber, N. C.; Sligar, S. G. *J. Biol. Chem.* **1994**, *269*, 4260–4266.

(6) (a) Spiro, T. G.; Li, X.-Y. In *Biological Applications of Raman Spectroscopy*; Spiro, T. G., Ed.; John Wiley & Sons: New York, 1988; Vol. 3, pp 1–39. (b) Yu, N.-T. In *Methods in Enzymology*; Hirs, C. H. W., Timasheff, S. N., Eds.; Academic Press: New York, 1986; Vol. 130, pp 350–409. (c) Kerr, E. A.; Yu, N.-T. In *Biological Applications of Raman Spectroscopy*; Spiro, T. G., Ed.; John Wiley & Sons: New York, 1988; Vol. 3, pp 39–97. (d) Kitagawa, T. In *Biological Applications of Raman Spectroscopy*; Spiro, T. G., Ed.; John Wiley & Sons: New York, 1988; Vol. 3, pp 97–133.

(7) Gunsalus, I. C.; Meeks, J. R.; Lipscomb, J. D.; Debrunner, P.; Munck, E. In *Molecular Mechanisms of Oxygen Activation*; Hayaishi, O., Ed.; Academic Press: New York, 1974; pp 559–613.

(8) (a) Yu, N. T.; Benko, B.; Kerr, E. A.; Gersonde, K. *Proc. Natl. Acad. Sci. U.S.A.* **1984**, *81*, 5106–5110. (b) Tanaka, T.; Yu, N. T.; Chang, C. K. *Biophys. J.* **1987**, *52*, 801–805. (c) Han, S.; Madden, J. F.; Siegel, L. M.; Spiro, T. G. *Biochemistry* **1989**, *28*, 5477–5485. (d) López-Garriga, J. L.; Oertling, W. A.; Kean, R. T.; Hoogland, H.; Wever, R.; Babcock, G. T. *Biochemistry* **1990**, *29*, 9387–9395. (e) Hu, S.; Treat, R. W.; Kincaid, J. R. *Biochemistry* **1993**, *32*, 10125–10130. (f) Al-Mustafa, J.; Kincaid, J. R. *Biochemistry* **1994**, *33*, 2191–2197. (g) Al-Mustafa, J.; Sykora, M.; Kincaid, J. R. *J. Biol. Chem.*, in press. (h) Rajani, C.; Kincaid, J. R. *J. Raman Spectrosc.*, in press.

For preparation of camphor-free P450cam, the native enzyme was passed successively over a Sephadex G-25 column equilibrated with 50 mM MOPS buffer (pH 7.4) and a Sephadex G-25 column equilibrated with 20 mM potassium phosphate (pH = 7.4) (KPi) containing 100 mM KCl.

The cyanide adducts of substrate-free P450cam were prepared by adding buffered 0.1 M KCN (final concentration of 50 mM) to 0.1 mM substrate-free P450cam in 100 mM KPi , with 100 mM KCl, pH = 7.4. The cyanide complex, kept in tightly closed vials at 4 °C, is stable for days.

The camphor-bound P450cam cyanide adduct was prepared by the addition of either an 8 mM stock solution of camphor (final concentration of 1 mM) to the P450cam-CN adduct or a 0.1 M KCN buffered solution (50 mM final concentration) to 0.1 mM P450cam in 100 mM KPi , with 100 mM KCl and 1 mM camphor, pH = 7.4.

Adamantanone-bound P450cam was prepared by passing the enzyme successively over a Sephadex G-25 column equilibrated with 50 mM MOPS buffer pH = 7.4 and Sephadex G-25 equilibrated with 100 mM KPi with 2 mM adamantanone and 200 mM KCl, pH = 7.4. The substrate-saturated enzyme was concentrated and stored in liquid nitrogen. Cyanide ligated P450cam saturated with adamantanone was prepared in the same way as described for the camphor-bound enzyme. Protein concentrations were determined by optical spectroscopy.^{9,10}

The isotopomeric cyanide adducts were prepared from different aliquots of the same protein solution and measured with identical instrumental conditions. The isotopically labeled cyanides (K^{13}CN , $\text{K}^{13}\text{C}^{15}\text{N}$, and $\text{K}^{13}\text{C}^{15}\text{N}$ at 99% enrichment) were obtained from Isotech Inc. (Miamisburg, OH).

The $^1\text{H}_2\text{O}/^2\text{H}_2\text{O}$ buffer exchange was carried out in a microconcentrator (Centricon-30). About 0.5 mL of the enzyme sample solution was added to the concentrator with 2.5 mL of the same buffer in $^2\text{H}_2\text{O}$. This solution was concentrated by centrifugation to 0.5 mL. This procedure was repeated 5 times. The total exchange time was approximately 16 h for substrate-free and 36 h for substrate-bound samples. Cyanide was added as buffered $^2\text{H}_2\text{O}$ solution.

Spectroscopic Measurements. The Resonance Raman spectra were acquired using a Spex 1269 spectrometer equipped with a Princeton Instruments ICCD-576 UV-enhanced detector, using a 442 mW notch filter (Kaiser Optical). The 441.7 nm excitation line was from a Linconix Model 4240 NB Helium Cadmium laser. The power used at the sample was 15 mW. The accumulation time for the spectra was commonly 5000–6000 s and the spectra were calibrated in the high- and low-frequency regions using fenchone. During the RR measurements the samples were kept in sealed short NMR tubes (5 mm diameter). The tubes were spun and cooled with a stream of cold nitrogen flowing over the illuminated region. Optical spectra were recorded before and after every RR measurement to ensure integrity of the sample.²⁴

Generation of Difference Spectra. The absolute spectra were white light and background corrected. Digital subtraction of the absolute spectra over the entire measured region (i.e., 200–800 cm^{-1} for low-frequency measurements) was performed using the facilities of Spectra Calc software. The subtraction was performed in such a way as to confirm the complete cancellation of intense porphyrin modes (e.g., $\nu_7 = 678 \text{ cm}^{-1}$). After subtraction, the difference spectrum was baseline corrected. The points selected for correction were out of the region where difference patterns were present. The simulated difference spectra were generated using programs described elsewhere.^{8,9}

Results

Substrate-Free Enzyme. The RR spectra of the substrate-free adducts of the various cyanide isotopomers are given in Figure 1. Owing to the presence of several heme deformation modes in this region, the modes associated with the FeCN fragment are not readily apparent. Thus, comparison of the different traces in Figure 1 reveals only small apparent isotope shifts and subtle intensity changes. Inasmuch as, in general, the heme modes are not expected to be sensitive to CN^- isotopic substitution, their frequencies and intensities presumably remain constant throughout the series and these modes can be expected

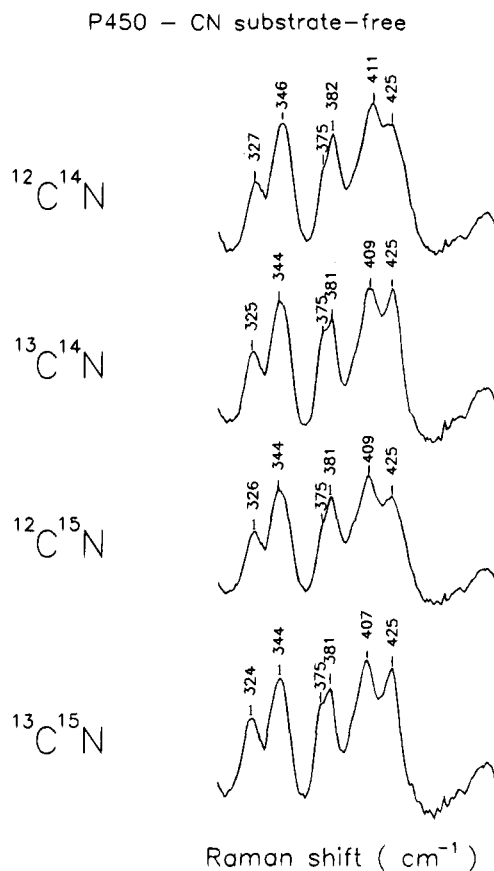


Figure 1. Low-frequency RR spectra of substrate-free P450cam-CN. Samples were prepared from 0.1 mM P450cam camphor-free in 100 mM KPi with 100 mM KCl, pH = 7.4, by addition of buffered 0.1 M KCN to a final concentration of 50 mM. Laser line 441.7 nm. Power at the sample 15 mW. Accumulation time 5000 s.

to cancel in the difference spectra. Ideally, the difference spectra should thus reveal only those modes associated with the FeCN fragment.

In Figure 2 are shown the set of possible difference spectra which can be generated by subtracting various pairs of absolute spectra. In the simplest situation it is expected that the FeCN fragment would give rise to two low-frequency modes: a $\nu(\text{Fe}-\text{C})$ stretch and a $\delta(\text{FeCN})$ bend. However, the complex difference patterns shown in Figure 2 suggest a more complicated situation. In fact, these experimental difference patterns can be satisfactorily simulated (Figure 3, Table 1) only if it is assumed that there are six modes in this region. Two of them (those located at 328 and 350 cm^{-1}) exhibit only very slight shifts and are attributed to low-frequency heme deformation modes which are vibrationally coupled to a mode at 343 cm^{-1} , which is associated with the FeCN fragment. At this point is important to point out that the absolute RR scattering cross section for the various modes is sensitive to many factors and, therefore, the derived relative intensities do not necessarily reflect the relative population of the two conformers.

Although the patterns are complex, and in certain cases the difference features are quite weak, it is satisfying that all six experimental difference patterns are fairly well reproduced by the set of derived parameters listed in Table 1. The fact that the derived isotopic shifts for the four modes associated with the FeCN fragment are consistent with those previously observed for similar systems (vide supra) also lends confidence to these derived values. We wish to emphasize that the distinctive patterns observed between 320 and 360 cm^{-1} in the six difference spectra could be adequately reproduced only by

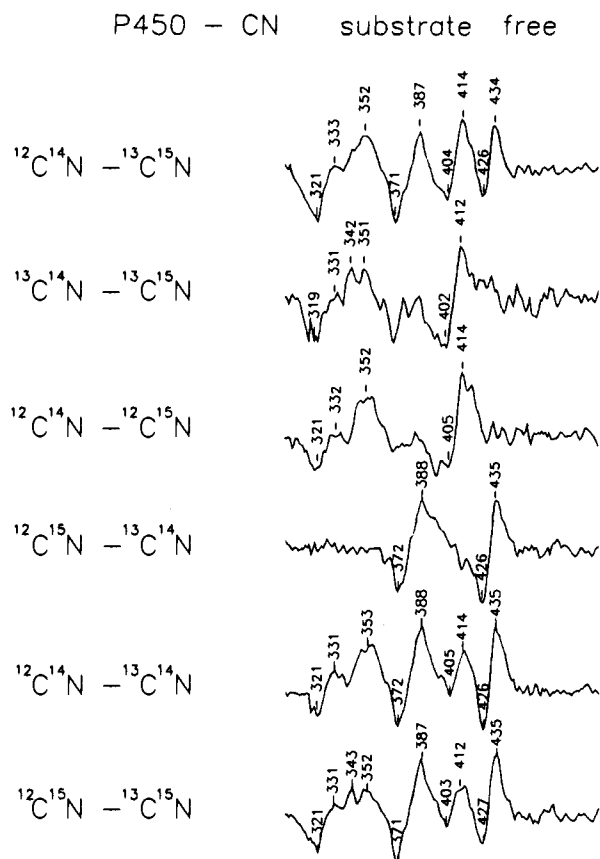


Figure 2. Experimental difference spectra for substrate-free P450cam-CN. These were generated by digital subtraction of the various spectra shown in Figure 1.

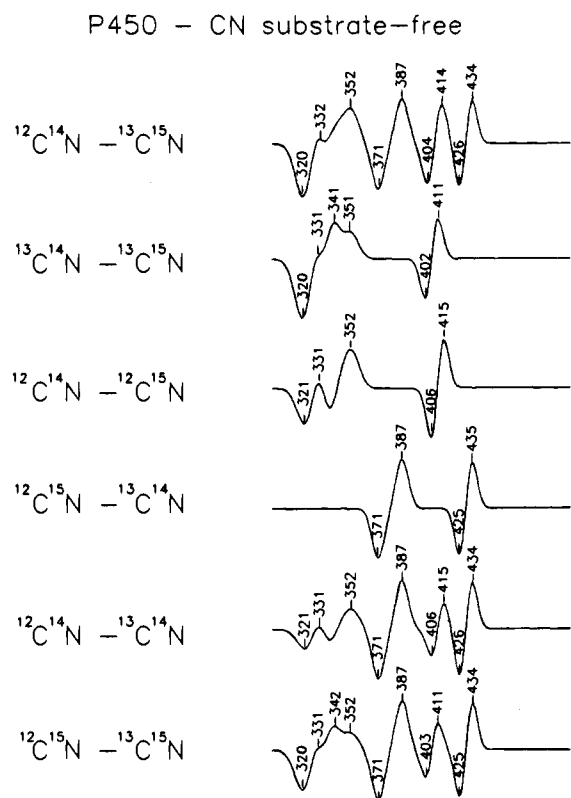


Figure 3. Simulated difference spectra for substrate-free P450cam-CN.

including the two modes at 328 and 350 cm^{-1} , both of which exhibited only small isotope shifts.

The simulation thus suggests that the CN^- ligand can bind

Table 1. Derived Frequencies for Isotope Sensitive Modes

P459-CN substrate free	$^{12}\text{C}^{14}\text{N}$	328	343	350	387	413	434
	$^{13}\text{C}^{14}\text{N}$	327	340	349	371	409	426
	$^{12}\text{C}^{15}\text{N}$	327	340	349	387	409	434
	$^{13}\text{C}^{15}\text{N}$	325	335	348	371	405	426
	fwhm ^a	18	16	16	12	12	10
	RI ^b	4	1.3	2.6	1	1	1
P450-CN camphor bound	$^{12}\text{C}^{14}\text{N}$		359		392	416	424
	$^{13}\text{C}^{14}\text{N}$		354		381	411	416
	$^{12}\text{C}^{15}\text{N}$		356		391	412	424
	$^{13}\text{C}^{15}\text{N}$		350		377	406	416
	fwhm ^a		12		16	16	12
	RI ^b		1		3	1.6	1
P450-CN adamantanone bound	$^{12}\text{C}^{14}\text{N}$		357		387	423	437
	$^{13}\text{C}^{14}\text{N}$		350		377	417	429
	$^{12}\text{C}^{15}\text{N}$		353		384	419	437
	$^{13}\text{C}^{15}\text{N}$		348		372	413	429
	fwhm ^a		12		18	16	10
	RI ^b		1.1		1	2	1

^a Full width at half maxima. ^b Relative intensities.

in two different geometries. Based on the above data and the previous studies mentioned earlier, one form is essentially linear exhibiting a monotonically shifting $\nu(\text{Fe}-\text{C})$ (413 cm^{-1}) at a higher frequency than the $\delta(\text{Fe}-\text{CN})$ bending mode (387 cm^{-1}) which has the characteristic "zigzag" pattern of isotopic shifts. The second conformer, apparently existing in a bent configuration, has vibrational properties which are characterized by a lower frequency (343 cm^{-1}), monotonically shifting mode and a higher frequency (434 cm^{-1}) mode which exhibits a characteristic zigzag pattern.

In an attempt to gain some insight into the nature of the factors which control ligand orientation, we have obtained RR spectra in the presence of $^1\text{H}_2\text{O}$ and $^2\text{H}_2\text{O}$. The absolute and difference spectra, as well as the simulated difference spectrum, are given in Figure 4. It should be pointed out that in order to precisely reproduce this difference pattern it was necessary to include two (presumably heme) modes whose frequencies are 372 and 402 cm^{-1} (in $^1\text{H}_2\text{O}$) and to increase the bandwidth slightly for the FeCN associated modes in the case of $^2\text{H}_2\text{O}$ (as listed in the caption for Figure 4). We note that similar $^2\text{H}_2\text{O}$ induced shifts for heme modes in this region have been reported for other oxidized heme proteins.¹¹ The 372 cm^{-1} mode is affected by $^2\text{H}_2\text{O}$ in the same way ($\sim 5 \text{ cm}^{-1}$) as the 379 cm^{-1} mode of metHb,^{11a} and the 402 cm^{-1} mode responds to $^1\text{H}_2\text{O}/^2\text{H}_2\text{O}$ exchange in a way similar to the 398 cm^{-1} mode of cytochrome *c*.^{11c} As can be seen in Figure 4 the experimental difference pattern is quite well reproduced by the simulation procedure, which yields derived shifts to higher frequency for both the $413 (7 \text{ cm}^{-1})$ and $343 \text{ cm}^{-1} (3.2 \text{ cm}^{-1})$ modes upon substitution of $^1\text{H}_2\text{O}$ for $^2\text{H}_2\text{O}$.

The Camphor-Bound Adduct. The RR spectra of the CN^- adducts of camphor-bound P-450cam are given in Figure 5. Though it can be noticed that there is a subtle manifestation of a "zigzag shift" influence on the data (spectra a and c having a similar shape, which is different from the shape of spectra b and d), it is not possible to identify modes associated with the FeCN fragment directly from these absolute spectra. However, the corresponding difference spectra, given in Figure 6a, are adequately simulated (Figure 6b) by assuming the presence of only four modes, whose parameters are listed in Table 1. In this case there is no need to include any heme macrocycle modes in the simulation, indicating that in the camphor-bound adduct the FeCN fragment is vibrationally isolated.

(11) (a) Feis, A.; Marzocchi, M. P.; Paoli, M.; Smulevich, G. *Biochemistry* **1994**, *33*, 4577-4583. (b) Sitter, A. J.; Shifflett, J. R.; Turner, J. J. *Biol. Chem.* **1988**, *263*, 13032. (c) Hildebrand, P.; Vanhecke, F.; Heibel, G.; Mauk, G. *Biochemistry* **1993**, *32*, 14158-14164.

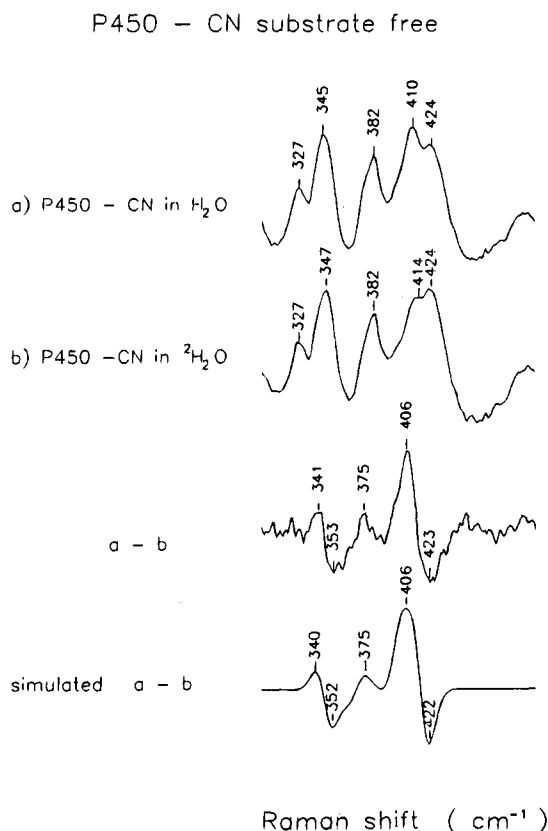


Figure 4. Low-frequency RR spectra of substrate-free P450cam-CN ($^1\text{H}_2\text{O}/^2\text{H}_2\text{O}$): (a) in $^1\text{H}_2\text{O}$ and (b) in $^2\text{H}_2\text{O}$ buffer, 100 mM KPi with 100 mM KCl. Laser line 441.7. Accumulation time 6000 s. The difference spectrum a-b is generated by digital subtraction of spectra a and b. The simulated difference spectrum was generated with the absolute values listed below. Spectrum a: absolute frequencies 343, 372, 402, 413 cm^{-1} ; full width at half maxima (fwhm) 16, 18, 20, 12 cm^{-1} ; relative intensities (RI) 2.6, 1, 5.3, 2. Spectrum b: absolute frequencies 346, 366, 399, 420 cm^{-1} ; full width at half maxima (fwhm) 18, 18, 20, 18 cm^{-1} ; relative intensities (RI) 3, 1, 2.6, 2.6.

As is clear from inspection of the data in Table 1, these experimental difference patterns are again adequately reproduced by assuming the existence of two conformers. The essentially linear conformer exhibits the $\nu(\text{FeC})$ and $\delta(\text{FeCN})$ modes at 424 and 392 cm^{-1} , respectively. The features identified at 359 and 424 cm^{-1} are assigned to the bent form.

It is interesting to note that, in contrast to the substrate-free system, we were unable to document any reproducible difference patterns upon $^1\text{H}_2\text{O}/^2\text{H}_2\text{O}$ exchange. While this suggests that, in the presence of substrate, the factors which gave rise to the $^1\text{H}_2\text{O}/^2\text{H}_2\text{O}$ effect shown in the substrate-free case are apparently eliminated or diminished (vide infra), we note that the S/N ratio of the difference patterns is much lower for the camphor-bound case.

Adamantanone-Bound Adduct. The experimental difference spectra for this adduct are given in Figure 7a. As can be seen by comparison with Figure 7b, the experimental difference pattern is well reproduced by the derived vibrational parameters of only four modes (given in Table 1). Again, both an essentially linear form and a bent form are indicated, the vibrational properties of which are similar to the corresponding forms observed in the substrate-free and camphor-bound forms.

Discussion

A. Computational Support for Mode Assignments. The simulation procedure strongly suggests that the experimentally observed difference patterns are the result of the presence of

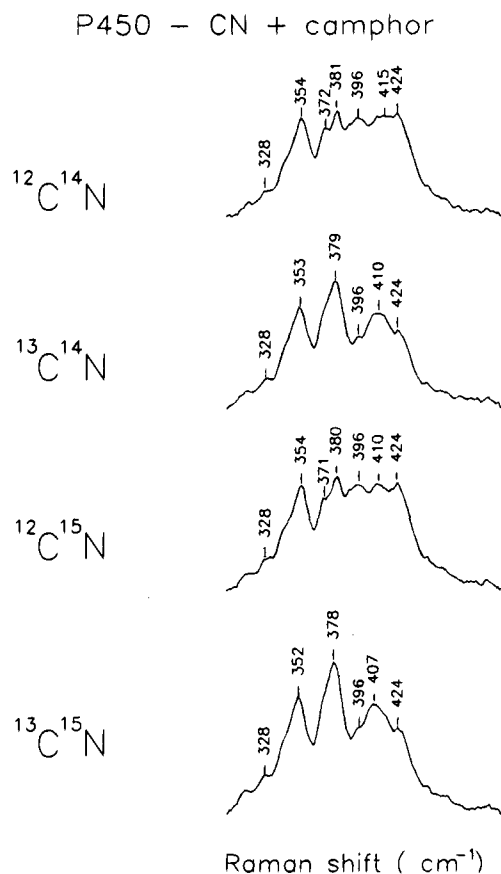


Figure 5. Low-frequency RR spectra of camphor-bound P450cam-CN. Samples were prepared from 0.1 mM P450cam in 100 mM KPi with 100 mM KCl and 1 mM camphor, pH = 7.4, by addition of buffered KCN to a final concentration of 50 mM. Laser line 441.7 nm. Power at the sample 15 mW. Accumulation time 6000 s.

four (cyanide) isotope-sensitive features, whose frequencies and approximate relative intensities are summarized in Table 1. In order to support the argument that these four features are associated with the two stretching and two bending modes of two conformers ("linear" and "bent"), normal mode calculations, using the familiar programs produced by Schachtschneider,¹² have been performed so as to determine the expected vibrational parameters for two such structures.

In conducting the normal mode calculations it was considered most reasonable to assume that any steric or electronic factors that are associated with substrate binding (or H-bonding changes) would have a greater effect on the geometry of the FeCN fragment and its associated force constants than on other fragments. Thus, in fitting the frequencies and isotopic shifts of the bent form, the geometries and force constants for the Fe-S and Fe-N_p fragments were held constant. The bond distances and angles of the basic model are given in Table 2 and are based on crystallographic data for ferric cytochrome P450 camphor.^{3a,b} Calculations were performed for the two separate conformers and the results for both are summarized in Table 2.

Considering first the "essentially linear" form, it must be pointed out that the activation of a second (i.e., bending) mode implies a slight distortion from a strictly linear, perpendicular geometry. Such distortion may arise from a slightly bent (i.e., $\angle\text{Fe}-\text{C}-\text{N} < 180^\circ$, $\angle\text{N}_p\text{FeC} = 90^\circ$) or slightly "tilted" (i.e., $\angle\text{Fe}-\text{C}-\text{N} = 180^\circ$, $\angle\text{N}_p\text{FeC} < 90^\circ$) geometry. As can be

(12) Schachtschneider, J. H.; Mortimer, F. S. *Vibrational Analysis of Polyatomic Molecules*; Technical Reports No. 231-61, Shell Development Co.: Emeryville, CA, 1964.

P450 - CN + camphor

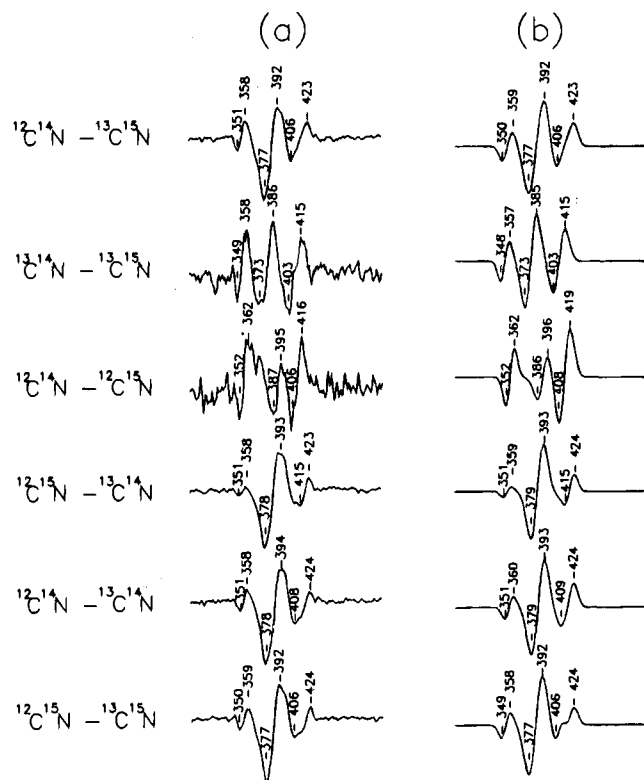


Figure 6. Difference spectra for camphor-bound P450cam-CN. Spectra were generated by digital subtraction (a) of various spectra shown in Figure 5 and simulated (b) by the parameters listed in Table 1.

seen by inspection of Table 2, the calculated frequencies and isotopic shifts can be well reproduced for either configuration. However, we note that the observed shifts of the stretching and bending modes (in opposite directions) upon replacement of camphor by the larger adamantanone arise kinematically (i.e., no force constant changes required) in the calculation for the bent distortion, but require force constant changes to reproduce in the calculation for the tilted form; i.e., using the force constants listed for the $180^\circ/85^\circ$ (camphor-bound) case, increasing the tilt angle did not reproduce the shifts observed for the adamantanone-bound form. Thus, the calculation supports the argument that the substrate-induced distortion involves bending rather than tilting. We note that the frequencies observed for the linear form of the substrate-free species could not be reproduced with any geometry tested using the force constants listed for the substrate-bound forms. However, only slight adjustments of the $S(\text{Fe}-\text{C})$ and $B(\text{FeCN})$ constants did give a good fit.

In discussing the calculations for the so-called "bent" form, it is useful to point out the significant differences in the vibrational parameters of this form relative to the "essentially linear" forms. First, it should be noted that the separation between the two isotopically sensitive modes is increased: ~ 350 and 430 cm^{-1} ($\sim 80 \text{ cm}^{-1}$) vs 420 and 390 cm^{-1} ($\sim 30 \text{ cm}^{-1}$). Most significantly, it is noted that the isotope shift patterns for the two modes are comparable for this form. Thus, the high-frequency mode of the linear form shifts purely monotonically and has a total ($^{12}\text{C}^{14}\text{N}^- - ^{13}\text{C}^{15}\text{N}^-$) shift much smaller than the corresponding bending mode, whereas in the case of the bent form, the shifts are comparable for the two modes.

As can be seen by inspection of the lower part of Table 2, this observed behavior is quite faithfully reproduced by the calculation. It should be emphasized that the essential differ-

P450 - CN + adamantanone

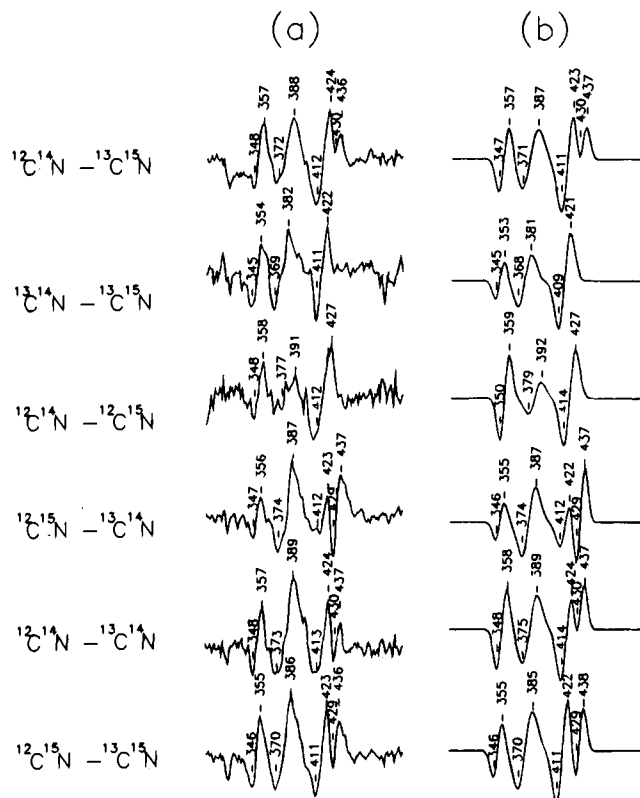


Figure 7. Difference spectra for adamantanone-bound P450cam-CN. Spectra were generated by digital subtraction (a) of various absolute spectra (not shown) recorded in identical conditions with the camphor-bound experiment, labeled as indicated, and then simulated (b) by the parameters listed in Table 1.

ences in the behavior observed for the two conformers can be reproduced merely by changing the values of only three force constants, all others being held constant. Thus, upon distortion of the FeCN fragment from linearity, the $S(\text{Fe}-\text{C})$, $B(\text{FeCN})$, and $S/S(\text{Fe}-\text{C}/\text{Fe}-\text{S})$ force constant values are lowered.

In contrast to the linear form case, it was not possible to reproduce the frequencies and isotope shifts of the substrate-free or adamantanone-bound forms merely by incorporating slight geometry changes (i.e., it was necessary to make force constant changes). While the differences between the camphor- and adamantanone-bound forms could be duplicated by changing only the $S(\text{Fe}-\text{C})$, the observed frequencies (and shifts) for the substrate-free derivative were most effectively reproduced with the parameters listed.

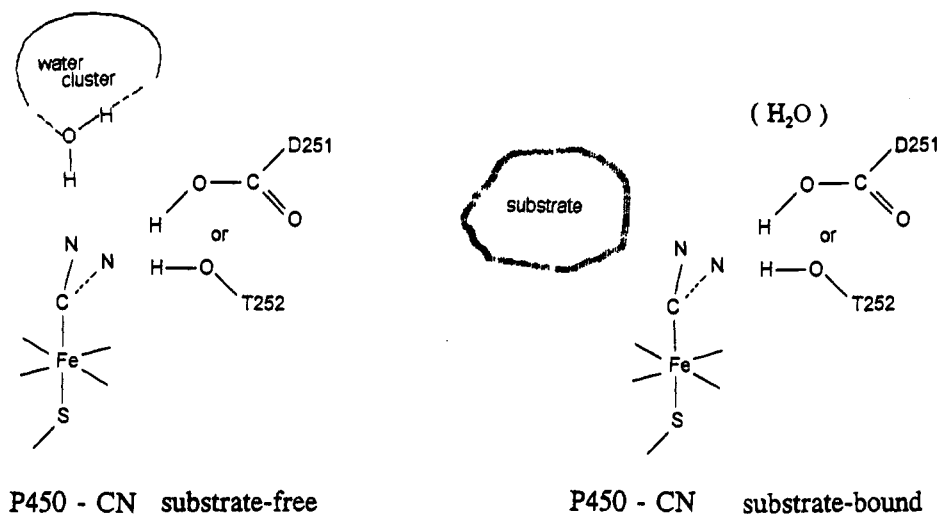
Special consideration is needed in comparing the observed and calculated results for the bent form of the substrate-free analogue. Thus, it is noted that while a "zigzag"-like shift pattern is calculated for this mode, the frequencies derived from the simulation imply a monotonic isotope shift pattern. The existence of a coupling interaction of this mode with the two heme modes in this region could easily give rise to this apparent discrepancy. Thus, the inherent frequencies of the FeCN associated mode for the $^{12}\text{C}^{14}\text{N}^-$ and $^{12}\text{C}^{15}\text{N}^-$ analogues would position it to interact more strongly with the higher frequency ($\sim 350 \text{ cm}^{-1}$) heme mode, while the inherent frequencies of this mode for the $^{13}\text{C}^{14}\text{N}^-$ and $^{13}\text{C}^{15}\text{N}^-$ analogues would position it to interact more strongly with the lower frequency ($\sim 328 \text{ cm}^{-1}$) heme mode. The net result of this interaction would thus be to cause the frequencies of the $^{13}\text{C}^{14}\text{N}^-$ and $^{12}\text{C}^{14}\text{N}^-$ isotopomers to lie closer together.

Finally, we would like to point out that it is possible to

Table 2. Calculated Frequencies (cm^{-1}) and Isotope Shifts^a

	G	1	2	3	4	5	6	7	8	9	calculated		observed		
linear ^c															
A	175 90	1.80	17.25	1.48	1.00	0.36	0.20	0.34	0.30	0.07	412.8	(4, 4, 8)	91, 21, 0 ^b	413	(4, 4, 8)
											384.0	(10, 2, 12)	3, 0, 85	384	(16, 0, 16)
											325.0	(1, 1, 3)	8, 81, 0	328	(1, 1, 3)
B	175 90	1.83	17.25	1.48	1.00	0.38	0.20	0.34	0.30	0.07	416.0	(4, 4, 8)	91, 21, 0	416	(5, 4, 10)
											393.0	(10, 1, 13)	3, 0, 86	392	(11, 1, 15)
											325.1	(1, 1, 2)	8, 82, 0	328	(0, 0, 0)
C	169 90	1.83	17.25	1.48	1.00	0.38	0.20	0.34	0.30	0.07	423.2	(6, 4, 10)	86, 14, 15	423	(6, 4, 10)
											387.4	(8, 3, 11)	7, 10, 69	387	(8, 3, 15)
											324.5	(1, 2, 3)	7, 79, 1	325	(0, 0, 0)
	180 85	1.83	17.25	1.48	1.00	0.38	0.20	0.34	0.30	0.03	418.0	(4, 4, 8)	84, 18, 7	416	(5, 4, 10)
											392.4	(10, 2, 12)	9, 4, 79	392	(11, 1, 15)
											325.4	(1, 1, 2)	8, 81, 0	325	(0, 0, 0)
180 80	1.83	17.25	1.48	1.00	0.38	0.20	0.34	0.30	0.03	419.2	(4, 4, 8)	82, 16, 8	423	(6, 4, 10)	
										392.0	(10, 3, 12)	9, 4, 79	387	(8, 3, 15)	
										325.4	(1, 1, 2)	8, 81, 0	325	(0, 0, 0)	
bent ^d															
D	155 90	1.40	17.25	1.48	1.00	0.33	0.20	0.34	0.10	0.07	425.1	(7, 2, 9)	68, 21, 21	424	(8, 0, 8)
											358.9	(5, 1, 6)	0, 40, 45	359	(5, 3, 9)
E	155 90	1.50	17.25	1.48	1.00	0.33	0.20	0.34	0.10	0.07	435.5	(8, 2, 10)	72, 18, 18	437	(8, 0, 8)
											359.0	(5, 2, 6)	0, 40, 46	357	(7, 4, 9)
F	150 90	1.35	17.25	1.48	1.00	0.30	0.20	0.34	0.02	0.07	435.0	(7, 2, 9)	69, 25, 13	434	(8, 0, 8)
											348.8	(5, 1, 6)	1, 43, 43	343	(3, 3, 8)

^a (i) A simplified 8 atom model was used; the iron atom is equally distant bound to four nitrogen atoms with equal mass (108 amu). For cysteine, the sulfur atom with 32 amu mass was considered. (ii) The sulfur atom was considered perpendicular to the porphyrin ring ($\angle S-Fe-N_p = 90^\circ$). The cyanide ligand was allowed to change geometry by bending, decreasing $\angle Fe-C-N$ (lower than 180°) or/and tilting, by decreasing $\angle N_p-Fe-C$ angle (lower than 90°). G column contains, in order, the bending and tilting angle (in deg) for each conformer. (iii) Used bond length (\AA): Cys-Fe = 2.20, Fe-C = 1.908, CN = 1.152, Fe-N_p = 2.05. (iiii) Used force constants: 1, $S(Fe-C)$, 2, $S(CN)$; 3, $S(Fe-S)$, 4, $S(Fe-N_p)$; 5, $B(FeCN)$, 6, $B(SFeC)$; 7, $S/S(FeC/CN)$; 8, $S/S(SFe/FeC)$; 9, $S/B(FeC/FeCN)$. The units are mdyn/\AA for stretching, S/S , and S/B interaction force constants and mdyn/rad^2 for bending force constant. ^b Calculated percent PED, listed in the order $S(Fe-C)$, $S(Fe-S)$, $B(FeCN)$. ^c Calculations assigned for "Essentially linear": (A) P450cam-CN substrate-free; (B) P450cam-CN camphor-bound; (C) P450cam-CN adamantanone-bound. ^d Calculations assigned for Bent: (D) P450cam-CN camphor-bound; (E) P450cam-CN adamantanone-bound; (F) P450cam-CN substrate-free.

**Figure 8.** Cytochrome P450cam-CN active site for substrate-free and substrate-bound complex.

reproduce the observed frequency changes between the linear and bent forms by allowing force constants other than $S(Fe-C)$, $B(FeCN)$, and $S/S(FeC/FeS)$ to also change (especially the $S(Fe-S)$ force constant). In fact, in permitting this, one can arrive at a set of calculated frequencies whose PED's are different from those obtained here and comparable to those calculated for the cyanide adduct of myeloperoxidase;^{8d} i.e., the low-frequency mode contained $\sim 30\%$ $S(Fe-C)$ whereas the present calculation indicates that the lower frequency mode contains almost no Fe-C stretching character. In the absence of any firm evidence that the Fe-S bond of the cyanide adduct is altered upon distortion of the FeCN fragment, we felt obligated to make the minimal force field changes reported here. However, further work would be required to determine which approach is more appropriate.

In summary, the vibrational parameters observed for both

forms are reliably reproduced assuming a basically static heme-thiolate framework and two sets of geometries for the FeCN fragment. The observed differences between the "essentially linear" and bent forms are those predicted from the calculation making (chemically realistic) changes in only three force constants. Furthermore, the frequency differences observed for the linear form modes between the camphor and adamantanone-bound derivatives are accurately modeled solely by a steric perturbation.

B. Structure and Functional Implications. 1. Origin of the Bent Form. The essential structural elements of the cytochrome P-450cam active site for both the substrate-free and substrate-bound forms are depicted in Figure 8. In the absence of substrate, the distal-side pocket is occupied by a cluster of water molecules, one of which (or an associated hydroxide ion) binds to the sixth coordination position of the heme iron to

stabilize the low-spin state. For the cyanide adduct of the substrate-free form, the sixth coordination position of the ferric ion is occupied by the cyanide ligand. Upon substrate binding, this cluster is eliminated and the iron assumes a high-spin configuration (in the absence of strong field ligands such as cyanide).

In addition to this substrate-induced change in spin state (which facilitates reduction of the ferric ion to the ferrous form^{1b}), attention has recently been focussed on potential structural elements which might facilitate heterolysis of the O–O bond,⁵ and an important role for the threonine-252 and aspartate-251 residues has been suggested, a key feature of which is the proposal that either the aspartate or (more likely) the threonine acts as a H-bond donor to the bound dioxygen as depicted in Figure 8. While convincing arguments for this proposal have been made on the basis of functional alterations of various recombinant proteins,^{5b,d} up to this time there has been reported no definitive spectroscopic evidence for such an interaction with an axial-bound heme ligand. As is discussed below, the spectroscopic behavior of the FeCN fragment of these cyanide adducts can provide additional information which is relevant to the proposed “charge relay” mechanism.

In order to clarify the structural interpretation of the spectroscopic data presented here, it is useful to briefly state the results of several related studies. First, it has been established by NMR¹³ and RR^{8f} studies that in those heme proteins containing distal-side residues which are capable of acting as H-bond donors to the bound axial ligand, the strength of the resultant H bond is greater in the case of the negatively charged CN⁻ ligand than for the corresponding (ferrous) CO adduct. For example, in the case of horseradish peroxidase, RR studies of the CO adduct reveal a hydrogen-bonding interaction of the bound CO with the protonated distal histidyl imidazole group. This H bond is broken and the imidazole deprotonated at pH near 7.¹⁴ However, the imidazole group of CN-bound HRP remains protonated up to pH 11, as has been shown by both RR^{8d,f} and NMR.¹³ Such effects demonstrate an advantage of the CN⁻ adducts (vs the CO adducts) for the investigation of distal-side hydrogen-bonding interactions.

Such differences between CO (or NO) and CN⁻ are also observed for the P450cam analogues. Thus, previous RR studies of the corresponding ferrous-CO^{4c} and ferric-NO⁴ⁱ adducts confirm the existence of only one conformer (strictly linear) for the substrate-free enzyme, while the CN⁻ adduct of the substrate-free enzyme studied in this report clearly may assume either an essentially linear or a bent conformation. Therefore, the most reasonable interpretation for the existence of the bent form in the case of the CN⁻ adduct is the formation of a hydrogen bond with an off-axis proton donor. This donor could be a particular fragment of the associated water cluster or an active site protein side chain such as the threonine or aspartate residues identified in the proposed “charge relay” mechanism.⁵

Further support for this argument is provided by the shifts observed in buffers prepared in ²H₂O (Figure 4). Before discussing the case at hand, it is important to point out that while the absence of an ¹H₂O/²H₂O induced shift does not

exclude the possibility that an H-bonding interaction exists,^{15a} the observation of such a shift does provide supporting evidence for an H-bonding interaction. In the present case, the lower frequency mode of the bent conformer shifts from 343 cm⁻¹ in ¹H₂O to 346 cm⁻¹ in ²H₂O buffer. This slight shift to higher frequency is similar to that seen in analogous systems. Thus, the coordinated dioxygen of oxyhemerythrin shifts up by 4 cm⁻¹ in ²H₂O^{15b} while a hydrogen-bonded Fe–O–Fe fragment of ribonucleotide reductase shifts up by 6 cm⁻¹ in ²H₂O.^{15c} Such shifts are reasonably attributed to slightly stronger bonds involving deuterons (relative to protons). In this case (the bent form), the threonine (or aspartate) exchangeable protons, as well as the water cluster protons, are replaced with deuterons.

At this point it is appropriate to comment on the ¹H₂O/²H₂O effect on the linear conformer and the insight it provides regarding the slight distortion evidenced by the activation of the bending mode. As can be seen in Figure 4, the stretching mode for this form shifts from 413 to 420 cm⁻¹, a shift comparable to that seen in other systems in which the fragment in question participates in a hydrogen-bonding interaction.^{15b,c} In the case of the linear conformer, the H-bond donor is almost certainly the cluster of water molecules which occupy the distal pocket of the substrate-free enzyme inasmuch as there are no nearby “on axis” H-bond donating protein residues.

Finally, it seems appropriate to point out that the frequencies observed for both conformers of the substrate-free form are in good agreement with those observed for the CN⁻ adducts of the other heme proteins, namely, the cyanide adducts of methemoglobin CTT III,^{8a} several hydroperoxidases,^{8d–h} and sulfite reductase.^{8c} Thus, RR studies have shown that in certain cases a linear conformer only is observed; e.g., cyano methemoglobin CTT III exhibits a monotonically shifting $\nu(\text{FeC})$ at 453 cm⁻¹ and a lower frequency band (412 cm⁻¹) which exhibits a “zigzag” isotope shift pattern. Some hydroperoxidase systems (known to possess a strong off-axis H-bond donor group) give rise to a bent conformer only,^{8d,e} while for others both conformers are possible.^{8c,f,g} Perhaps the most relevant previous RR study involves the CN⁻ adducts of sulfite reductase, which, like cytochrome P450cam, possesses a trans-iron–thiolate linkage.^{8c} In that case, again clear evidence was obtained for the existence of two conformers, with the linear form having the $\nu(\text{Fe–C})$ and $\delta(\text{FeCN})$ modes at 451 and 390 cm⁻¹, respectively. The corresponding frequencies for the bent conformer were 352 and 451 cm⁻¹.

In summary of this section, the RR data for the substrate-free enzyme reveal the presence of both a linear and a bent conformer, both of which exhibit the expected characteristic isotopic shift patterns and both of which are apparently in contact with a distal-side hydrogen bond donor which gives rise to the ¹H₂O/²H₂O sensitivity of both conformers. While the H-bond donor to the essentially linear form is most reasonably identified as the well-known distal pocket water cluster, a presumably off-axis donor forms a hydrogen bond to the bent conformer. This off-axis donor could be simply another region of the water cluster, or the threonine-252 or aspartate-251 residues. The fact that the ¹H₂O/²H₂O sensitivity is not detected in the substrate-bound form (vide infra) suggests that the water cluster of the substrate-free form serves as the H-bond donor to both conformers.

2. Effect of Substrate Binding. The spectroscopic changes observed upon substrate binding are quite consistent with those expected, given the structural interpretation outlined above for

(13) (a) Morishima, S. O.; Ogawa, S.; Inubushi, T.; Yonezawa, T.; Iizuka, T. *Biochemistry* **1977**, *16*, 5109–5114. (b) de Ropp, J. S.; La Mar, G. N.; Smith, K. M.; Langry, K. C. *J. Am. Chem. Soc.* **1984**, *106*, 4438–4444. (c) Thanabal, V.; de Ropp, J. S.; La Mar, G. N. *J. Am. Chem. Soc.* **1987**, *109*, 7516–7525. (d) Thanabal, V.; de Ropp, J. S.; La Mar, G. N. *J. Am. Chem. Soc.* **1988**, *110*, 3027–3035. (e) Morishima, I.; Inubushi, T.; Neya, S.; Ogawa, S.; Yonezawa, T. *Biochem. Biophys. Res. Commun.* **1977**, *78*, 739–746. (f) Behere, D. V.; Gonzalez-Vergara, E.; Goff, H. M. *Biochim. Biophys. Acta* **1985**, *632*, 319–325.

(14) Evangelista-Kirkup, R.; Smulevich, G.; Spiro, T. G. *Biochemistry* **1986**, *25*, 4420–4425.

(15) (a) Jeyarajah, S.; Proniewicz, L. M.; Bronder, H.; Kincaid, J. R. *J. Biol. Chem.* **1994**, *269*, 31047–31050. (b) Shiemke, A. K.; Loehr, T. M.; Sanders-Loehr, J. *J. Am. Chem. Soc.* **1986**, *108*, 2437–2443. (c) Sjöberg, B. M.; Loehr, T. M.; Sanders-Loehr, J. *Biochemistry* **1982**, *21*, 96–102.

the substrate-free enzyme. Considering first the vibrational behavior of the essentially linear form, it is noted that the $^1\text{H}_2\text{O}/^2\text{H}_2\text{O}$ shift is apparently abolished or drastically diminished for the substrate-bound form. This is obviously what is expected given that the distal pocket water cluster is eliminated upon substrate binding.^{3b} In fact, the results of ^{15}N NMR studies of the cyanide adduct of P450cam are also consistent with these RR results. Thus, the ^{15}N NMR resonance is observed at 423 ppm for the substrate-free form, a position which is comparable to that observed for various peroxidases, whose distal pockets are known to possess H-bond donors.^{2g} Upon substrate binding to P450cam the ^{15}N resonance shifts to 500 ppm. As the authors of the ^{15}N -NMR work point out, the ^{15}N -resonance shift (from 423 to 500 ppm) could result from several factors, one of which is a decreased H-bonding interaction.^{13e,f} While the ^{15}N -NMR data are not inconsistent with RR data, caution is required in comparing the two sets, because the ^{15}N -NMR signal is apparently an averaged signal of the two conformers whose RR signals are distinct.

It can be seen from inspection of Table 1 that the linear form frequencies are sensitive to substrate size with $\nu(\text{Fe}-\text{C})$ and $\delta(\text{FeCN})$ occurring at 416 and 392 cm^{-1} for the camphor-bound derivative and at 426 and 387 cm^{-1} for the adamantanone-bound enzyme. These changes are, in fact, predicted by the NCA calculations summarized in Table 2. Thus, only small changes in several force constants associated with the FeCN fragment are required to account for the difference observed between the substrate-free and the camphor-bound enzyme. These force constant changes are reasonable, given the fact that the substrate-free form participates in a hydrogen-bonding interaction which is decreased substantially upon substrate binding. It is especially satisfying that the sensitivity to substrate size is adequately duplicated by pure steric factors. Thus, the observed differences between the two substrate-bound forms are accurately reproduced merely by decreasing the FeCN angle in the case of the larger substrate without the need to change any force constant values.

As a final point regarding the substrate-bound linear form, it is important to point out that this sensitivity to substrate size observed for the linear form of CN^- adducts is directly analogous to that seen for other linear FeXY fragments of cytochrome P450cam. Thus, for both the ferrous- CO^{4c} and ferric- NO^{4i} systems the $\nu(\text{Fe}-\text{C})$ and $\nu(\text{Fe}-\text{N})$ were observed to differ between the camphor- and adamantanone-bound forms.

The persistence of the bent conformer in the substrate-bound form is of interest with respect to the recently proposed "charge relay" mechanism.⁵ As stated earlier, in the substrate-free form

this conformer arises as a consequence of off-axis hydrogen bonding. In the substrate-bound form, such a distortion may be induced either by off-axis hydrogen bonding or by steric interactions with the bound substrate. In the absence of a demonstrated $^1\text{H}_2\text{O}/^2\text{H}_2\text{O}$ effect, there is no evidence for an H-bonding interaction. In addition, one of the bent form modes is sensitive to substrate size, shifting from 424 cm^{-1} in the camphor-bound form to 437 cm^{-1} for the adamantanone-bound derivative form. Thus, while the absence of an $^1\text{H}_2\text{O}/^2\text{H}_2\text{O}$ effect cannot exclude the possibility of an off-axis H-bonding interaction (Thr-251 or Asp-251), this absence, together with the observed sensitivity to substrate size, is more consistent with the interpretation that steric factors are responsible for generating the bent configuration in the substrate-bound forms.

Conclusions

The RR studies presented here illustrate the advantage of CN^- as an exogenous ligand for probing distal pocket hydrogen bonding interactions in heme proteins. The results confirm the existence of both an essentially linear and a bent conformer whose sensitivities to substrate size and participation in hydrogen bonding with distal pocket donors are effectively monitored by the vibrational signatures of the two forms. In the substrate-free form, based on observed sensitivities to $^1\text{H}_2\text{O}/^2\text{H}_2\text{O}$ exchange, both conformers are apparently H-bonded to two different regions of the well-known water cluster that occupies the active site. The apparent absence of $^1\text{H}_2\text{O}/^2\text{H}_2\text{O}$ sensitivity in the substrate-bound forms, coupled with the sensitivity of modes of both conformers to substrate size, suggests that the apparently large off-axis distortion of the bent conformer arises as a consequence of steric interactions with bound substrate rather than from a hydrogen-bonding interaction with an off-axis donor.

Acknowledgment. This work was supported by a grant from the National Institutes of Health (DK 35153). The authors are thankful to Professor S. Sligar of the University of Illinois at Urbana-Champaign for the supply of *Pseudomonas putida* ATCC 29607 strain. We are especially grateful to Professor D. Noel of Marquette University for his careful guidance during the initial grow of bacterial culture and to J. Harper of the University of Wisconsin at Madison biochemistry pilot plant for his assistance during the large scale bacterial growth procedures. We are sincerely thankful to Dr. K. Czarniecki for his advice during the RR measurements and Mr. M. Sykora for his guidance during the computational work.

JA942818O